Molecular Biology of the Cell
Vol. 18, 4750–4761, December 2007

Myosin VI Is Required for Targeted Membrane Transport during Cytokinesis[D] [V]

Susan D. Arden,* Claudia Puri,* Josephine Sui-Yan Au,† John Kendrick-Jones,† and Folma Buss*

*Cambridge Institute for Medical Research, University of Cambridge, Cambridge CB2 2XY, United Kingdom; and †Medical Research Council Laboratory of Molecular Biology, Cambridge CB2 2QH, United Kingdom

Submitted February 15, 2007; Revised August 24, 2007; Accepted September 6, 2007
Monitoring Editor: Erika Holzbaur

Myosin VI plays important roles in endocytic and exocytic membrane-trafficking pathways in cells. Because recent work has highlighted the importance of targeted membrane transport during cytokinesis, we investigated whether myosin VI plays a role in this process during cell division. In dividing cells, myosin VI undergoes dramatic changes in localization: in prophase, myosin VI is recruited to the spindle poles; and in cytokinesis, myosin VI is targeted to the walls of the ingressing cleavage furrow, with a dramatic concentration in the midbody region. Furthermore, myosin VI is present on vesicles moving into and out of the cytoplasmic bridge connecting the two daughter cells. Inhibition of myosin VI activity by small interfering RNA (siRNA)-mediated knockdown or by overexpression of dominant-negative myosin VI tail leads to a delay in metaphase progression and a defect in cytokinesis. GAIP-interacting protein COOH terminus (GIPC), a myosin VI binding partner, is associated with the function(s) of myosin VI in dividing cells. Loss of GIPC in siRNA knockdown cells results in a more than fourfold increase in the number of multinucleated cells. Our results suggest that myosin VI has novel functions in mitosis and that it plays an essential role in targeted membrane transport during cytokinesis.

INTRODUCTION

When a single cell divides into two daughter cells, the chromosomes are segregated in mitosis, and then the cytoplasm and the plasma membrane are divided during cytokinesis to complete the cell cycle (Scholey *et al*., 2003). The process of cytokinesis is driven by the formation and constriction of an actomyosin II contractile ring and by targeted membrane addition (Glotzer, 2005). Membrane delivery is first required during cleavage furrow ingression to increase the surface area of the two daughter cells and later during the abscission process to seal the two newly formed cells (Strickland and Burgess, 2004; Albertson *et al*., 2005). Although membrane vesicles delivered into the cleavage furrow were thought to be derived from the secretory pathway (Skop *et al*., 2001), endocytosis and membrane recycling have also now been shown to be required for cytokinesis (Gerald *et al*., 2001; Schweitzer and D'Souza-Schorey, 2002; Fielding *et al*., 2005; Wilson *et al*., 2005). Endocytosis resumes during late cytokinesis and endocytic vesicles or vesicles from the recycling compartment are transported into the midbody region of the cleavage furrow (Schweitzer *et al*., 2005).

Because myosin VI is an actin-based motor protein involved in endocytic and exocytic membrane-trafficking pathways in interphase cells (Buss *et al*., 2004), we decided to test whether it was involved in cytokinesis in dividing cells. An increasing number of proteins associated with the actin and microtubule cytoskeleton and with membrane-trafficking pathways have been shown to play a role in cytokinesis. In a recent proteomic study by Skop *et al*. (2004), 160 candidate midbody proteins were identified, including myosin VI and its binding partner GAIP-interacting protein COOH terminus (GIPC). Furthermore, functional studies in *Caenorhabditis elegans* using RNA interference showed that both proteins display defects in germline cytokinesis (STE/GON) (Skop *et al*., 2004).

Myosin VI is a retrograde motor because, unlike all the other classes of myosins, it moves toward the minus end of actin filaments (Wells *et al*., 1999); therefore, it is expected to have unique and distinct intracellular functions. The targeting and functions of myosin VI at different intracellular locations involve a variety of different binding partners such as disabled-2 (Morris *et al*., 2002), GIPC (Bunn *et al*., 1999), and optineurin (Sahlender *et al*., 2005), and they also require binding to phosphatidylinositol 4,5-bisphosphate (PIP_2) in the plasma membrane (Spudich *et al*., 2007). GIPC is a postsynaptic density 95/disc-large/zona occludens domain-containing protein that interacts with myosin VI and with the cytoplasmic domains of several transmembrane receptors at the plasma membrane, where it may regulate endocytic receptor trafficking or intracellular signaling (De Vries *et al*., 1998).

In this study, we examined the role of myosin VI and its binding partner GIPC during cell division in mammalian cells. In prophase in early mitosis, myosin VI is present in the pericentriolar region. At the onset of cytokinesis, myosin VI is recruited to the contractile ring in the cleavage furrow, colocalizing with actin and myosin II; and after ingression, it is found in the region of the midbody, where it colocalizes

This article was published online ahead of print in *MBC in Press* (http://www.molbiolcell.org/cgi/doi/10.1091/mbc.E07–02–0127) on September 19, 2007.

[D] [V] The online version of this article contains supplemental material at *MBC Online* (http://www.molbiolcell.org).

Address correspondence to: Folma Buss (fb1@mole.bio.cam.ac.uk).

with GIPC. In time-lapse video microscopy, myosin VI can be seen associated with vesicles transported into and out of the midbody region, suggesting that it is involved in membrane trafficking during cytokinesis. Only the full-length "active" myosin VI but not the "nonfunctional" tail domain is targeted into the cleavage furrow and midbody. Overexpression of this dominant-negative tail inhibits delivery of vesicles containing the transferrin receptor (TfR) into the midbody region, and it results in multinucleated cells. In addition depletion of myosin VI or its binding partner GIPC, by using small interfering RNA (siRNA), leads to defects in cytokinesis. Furthermore, loss of myosin VI in KD cells causes a dramatic delay in progression through metaphase and in chromosome alignment.

These results highlight for the first time a role for myosin VI in the progression of mitotic cells through metaphase and demonstrate that myosin VI plays an important role in membrane trafficking events during cytokinesis.

MATERIALS AND METHODS

Antibodies

The following antibodies were used: a rabbit antibody to myosin VI (Buss *et al*., 1998), a rabbit antibody to calf thymus nonmuscle myosin II (Drenckhahn *et al*., 1983), a monoclonal antibody (mAb) to green fluorescent protein (GFP) (Q-biogen, Cambridge, United Kingdom), a polyclonal antibody to GFP (Molecular Probes, Leiden, The Netherlands); a mAb to α-tubulin (Sigma, Gillingham, United Kingdom), a mAb to transferrin receptor (Zymed, Cambridge BioScience, Cambridge, United Kingdom), and a rabbit polyclonal antibody to GIPC and a rabbit antibody to actin (Sigma). Rhodamine-coupled phalloidin (Sigma) was used to visualize F-actin filaments in immunofluorescence.

Cell Culture and Transfection

HeLa cells were cultured and transfected as described previously (Sahlender *et al*., 2005). After 16–18 h, the cells were either used for live cell imaging or they were fixed for immunofluorescence. Madin Darby canine kidney (MDCK) II cells were cultured in DMEM containing 10% (vol/vol) fetal calf serum, 2 mM L-glutamine, 100 U/ml penicillin, and 0.1 mg/ml streptomycin. Myosin VI or the tail domain tagged with GFP at the N terminus was cloned into the ΔpMEP4 vector (Warner *et al*., 2003). Protein expression was induced for 24 h with 100 μM $ZnCl_2$. For selection of stable MDCK cell lines, MDCK cells were transfected as described above and selected with 200 μg/ml hygromycin (Roche Diagnostics, Lewes, United Kingdom). Single clones were isolated, and the population of highly expressing cells enriched by fluorescence-activated cell sorting. Immunoblotting of stable cell lines showed that the concentration of expressed protein was at least equal to that of endogenous myosin VI (Au *et al*., 2007).

Knockdown of Myosin VI and GIPC by siRNA

siRNA knockdown experiments were performed as described previously (Sahlender *et al*., 2005). "On target Plus" SMARTpools designed and supplied by Dharmacon (Cramlington, United Kingdom) were used for knock down of myosin VI and GIPC. To perform siRNA-rescue experiments, three silent point mutations were made in the target sequence of one of the myosin VI SMARTpool oligos using QuikChange (Stratagene, Amsterdam, The Netherlands). A stable HeLa cell line was generated expressing GFP-tagged mutated siRNA-resistant myosin VI by using pIRESneo2 (Clontech-Takara BioEurope, Saint-Germain-en-Laye, France).

Indirect Immunofluorescence Microscopy

HeLa and MDCK cells were processed for immunofluorescence microscopy as described previously (Buss *et al*., 2001). To remove cytosolic proteins before fixation, MDCK cells expressing GFP-myosin VI or GFP-tail were prepermeabilized with 0.05% saponin in cytosol buffer (Morris and Cooper, 2001). Cells were analyzed and photographed using a Zeiss LSM 510 confocal microscope (Carl Zeiss, Welwyn Garden City, United Kingdom).

Fluorescence Live Cell Microscopy

For time-lapse fluorescence microscopy, MDCK cells expressing GFP-myosin VI were grown on 25-mm-diameter glass coverslips. Images were acquired with a 63× objective and a spinning disk confocal head (PerkinElmer-Cetus, Beaconsfield, United Kingdom) coupled to Zeiss Axiovert 135TV fluorescence microscope. Images were captured with ORCA-ER camera (Hamamatsu, Bridgewater, NJ) controlled by the UltraView imaging software (PerkinElmer-Cetus). Fluorescence images were acquired every 10 s and processed using ImageJ software (http://rsb.info.nih.gov/ij/).

Differential Interference Contrast (DIC) Live Cell Microscopy

For time lapse DIC microscopy control or knockdown (KD) HeLa cells were grown on 25-mm round coverslips that were mounted in an Attofluor cell chamber (Molecular Probes), which was filled with CO_2-independent medium (Invitrogen, Paisley, United Kingdom) and placed in a heated stage at 37°C on a Zeiss Axiovert 200M microscope (Carl Zeiss). DIC images were acquired every 2 min with Openlab and analyzed using Velocity software (Improvision, Coventry, United Kingdom).

Whole Mount Immunocytochemistry

Whole mount immunocytochemistry was performed as described previously (Stoorvogel *et al*., 1996; van Dam and Stoorvogel, 2002). HeLa cells were cultured overnight on Formvar carbon-coated gold grids mounted on glass coverslips. The cells were washed with ice-cold phosphate-buffered saline (PBS), and cytosolic proteins were extracted with PBS containing 1 mM EGTA, 0.5 mM $MgCl_2$, and 0.5 mg/ml saponin (Sigma Chemical, Poole, Dorset, United Kingdom) before fixation with 1% paraformaldehyde at 4° for 1 h. The cells were then incubated in blocking buffer (PBS, 0.5 mg/ml saponin, 20 mM glycine, 0.1% cold water fish gelatin, and 0.02% NaN_3) before immunolabeling (Slot *et al*., 1991) with a polyclonal antibody to myosin VI tail (Buss *et al*., 1998) followed by protein A 10-nm gold.

RESULTS

Localization of Myosin VI in Dividing Cells

We have shown that in interphase cells myosin VI is present in membrane ruffles at the plasma membrane, in the perinuclear region at or around the Golgi complex, and in vesicles throughout the cell (Buss *et al*., 1998; Buss *et al*., 2001; Warner *et al*., 2003). To investigate the localization of myosin VI in dividing cells, we immunostained MDCK cells with different myosin VI tail antibodies and we also examined stable MDCK cell lines expressing GFP-tagged myosin VI. Both approaches showed that at the onset of mitosis, during prophase and prometaphase, myosin VI is present in a vesicular, punctate staining pattern concentrated at the centrosome/spindle poles (Figure 1A, a–c, and B, g–i). In late anaphase/early telophase, myosin VI is recruited to the plasma membrane surrounding the ingressing cleavage furrow (Figures 3A and 4, a–c), and in later stages of cytokinesis, it is concentrated on either side of the midbody region (Figures 1A, d–f, and B, j–l; 2; 3, A–C; and 4, d–f). This very distinct recruitment of myosin VI to the spindle poles and the cleavage furrow and subsequently to the cytoplasmic bridge on either side of the midbody during cytokinesis was observed in immunofluorescence microscopy initially with different affinity-purified antibodies to myosin VI and then confirmed by expression of full-length GFP-tagged myosin VI (Figure 1B, g–l). To obtain higher resolution images of myosin VI in the midbody region, we performed whole mount immunoelectron microscopy on HeLa cells grown on Formvar carbon-coated gold grids. In this method, cytosolic proteins were removed before fixation and labeling with our rabbit polyclonal antibody to myosin VI tail. Consistent with the immunofluorescence data myosin VI is present along cytoskeletal structures on either side of the very electron-dense area of the midbody (Figure 2a). Enlarged images highlight the association of myosin VI with small intracellular vesicular structures of ~50 nm (Figure 2, b–d, arrows) and with fibrous cytoskeletal elements.

Four different splice variants of myosin VI either containing no insert, a small insert, a large insert, or both inserts in the tail domain are expressed in mammalian cells in a tissue-specific manner. In polarized MDCK cells, all myosin VI isoforms except the isoform with the small insert are expressed. Whereas the presence of the large insert seems to

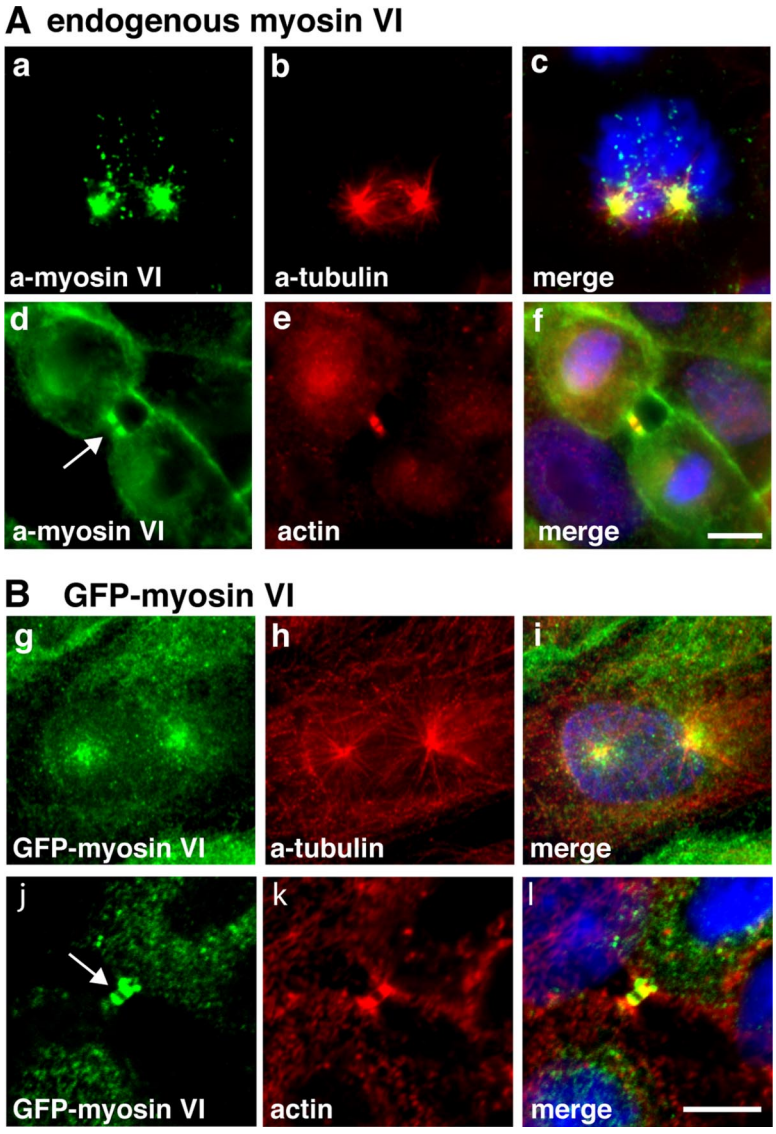

Figure 1. In mitotic cells myosin VI is associated with spindle poles in prophase and with the cleavage furrow during cytokinesis. (A) Endogenous myosin VI in MDCK cells was localized using a polyclonal myosin VI tail antibody (a and d). Double labeling with a monoclonal α-tubulin antibody (b) reveals that myosin VI is recruited to spindle poles in prophase and labeling F-actin with Rhodamine-phalloidin (e) highlights the presence of myosin VI in the cytoplasmic bridge between two daughter cells during cytokinesis (d) (arrow). Stable MDCK cells expressing full-length GFP-tagged myosin VI were either stained with GFP-antibody (g and j) or with α-tubulin antibody (h) or for F-actin with Rhodamine-phalloidin (k). GFP-myosin VI is recruited to the spindle poles in prophase (g) and to the midbody region in late cytokinesis (j) (arrow). The merged images together with the DNA stain in blue are shown in (c, f, i, and l). Bars, 10 μm.

increase the affinity of myosin VI for clathrin-coated endocytic structures (Spudich *et al*., 2007), the no-insert isoform is important for protein sorting in the exocytic pathway, leading to delivery to the basolateral domain in polarized epithelial cells (Au *et al*., 2007). All three myosin VI isoforms that are expressed in MDCK cells show the same localization in mitotic cells, indicating that in contrast to the localization of myosin VI isoforms in interphase cells, the inserts do not seem to play a role in differential targeting of myosin VI in mitotic cells (data not shown).

Myosin VI Is Present on Vesicular Structures Trafficking Into and Out of the Midbody Region

During cytokinesis, constriction of the cleavage furrow requires an increase in plasma membrane surface area. This is achieved by inserting new membrane into the cleavage furrow, which is either derived from the secretory or endocytic pathways. In interphase cells myosin VI is associated with endocytic and exocytic vesicles and the Golgi complex (Buss *et al*., 1998; Warner *et al*., 2003). Therefore, to explore whether myosin VI plays a role in directing membrane vesicles into the cleavage furrow, we used time-lapse video microscopy on MDCK cells stably expressing GFP-myosin VI. The dynamic behavior of myosin VI tagged with GFP during cytokinesis can be seen in still images in Figure 3. At the onset of cytokinesis, myosin VI is recruited and concentrated in the region of the plasma membrane, where the actin/myosin II contractile ring is being assembled (Figure 4) and the plasma membrane is starting to invaginate (Figure 3A and Supplemental Movie 1). During cleavage furrow ingression, myosin VI becomes very concentrated in the narrow cytoplasmic bridge on either side of the midbody. At the end of cytokinesis, myosin VI is gradually lost from the midbody region. In addition to the concentration of myosin VI in the cleavage furrow, we observed the recruitment of myosin VI to the plasma membrane outside the cleavage furrow and to punctate structures in the polar regions surrounding the spindle poles, which are most likely membrane vesicles (Supplemental Movie 1). Myosin VI is present on punctate structures that are moving from both daughter cells into the cytoplasmic bridge as shown on selected frames in Figure 3B (Supplemental Movie 2). In the left daughter cell, a small myosin VI-containing structure (highlighted by a arrow) is budding from a larger fluorescent structure before moving

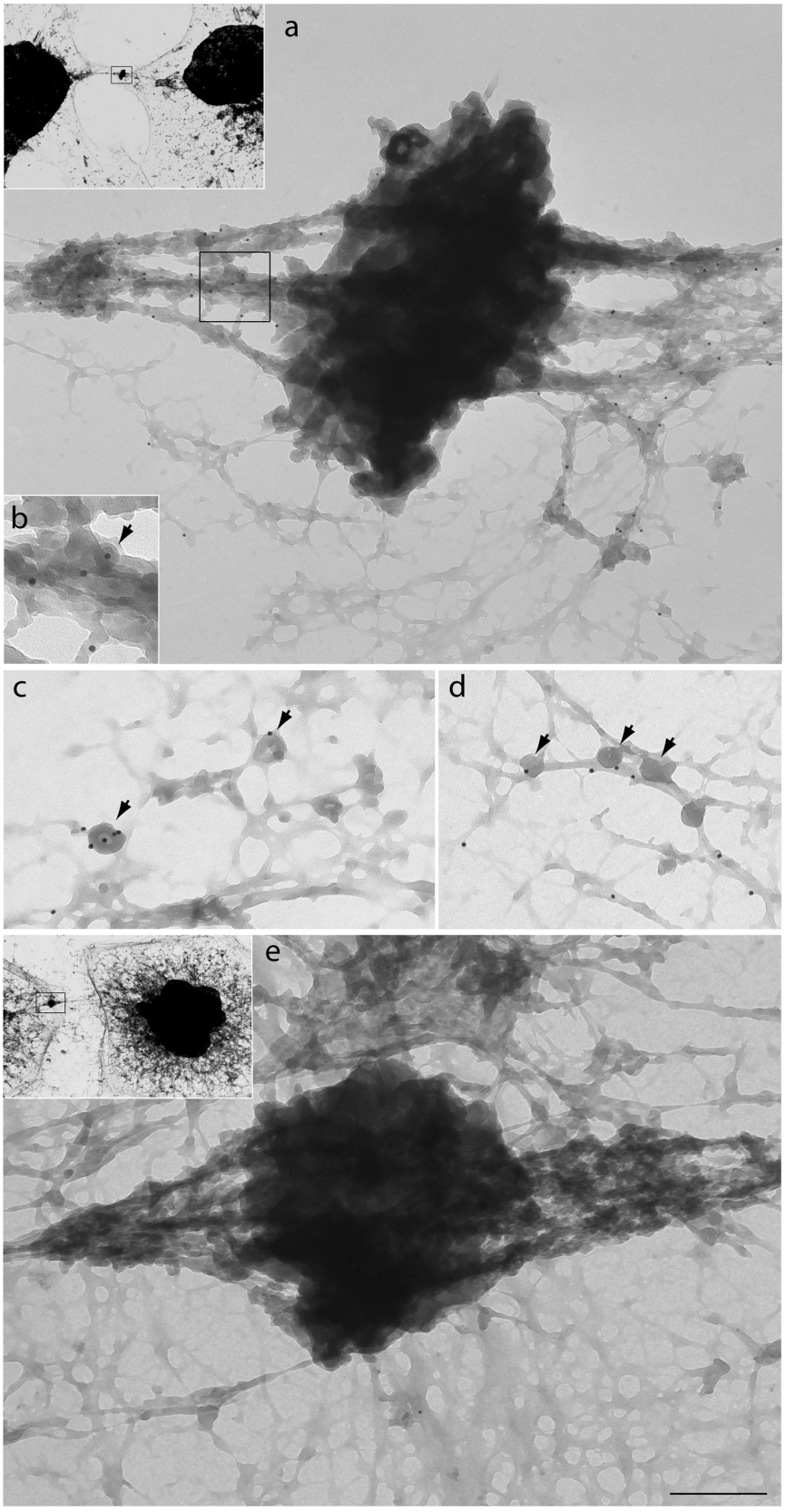

Figure 2. Immunoelectron microscopy localizes myosin VI to the intercellular bridge on either side of the midbody. The localization of myosin VI at the ultrastructural level was visualized in HeLa cells grown on grids that were saponin extracted and then fixed and stained for immunoelectron microscopy with our polyclonal antibodies to myosin VI tail followed by protein A 10-nm gold. Myosin VI is concentrated along cytoskeletal elements on either side of the dark midbody (a) and is associated with fibrous structures and vesicles of ~50 nm (arrows highlight vesicles in b–d). A control picture in which grids were incubated with protein A gold only is shown in e. Insets show lower magnification pictures (1000× of original) of cells from which regions were enlarged in a and e. Bar (in e) represents 375 nm (a), 150 nm (b), 200 nm (c), 300 nm (d), and 375 nm (e).

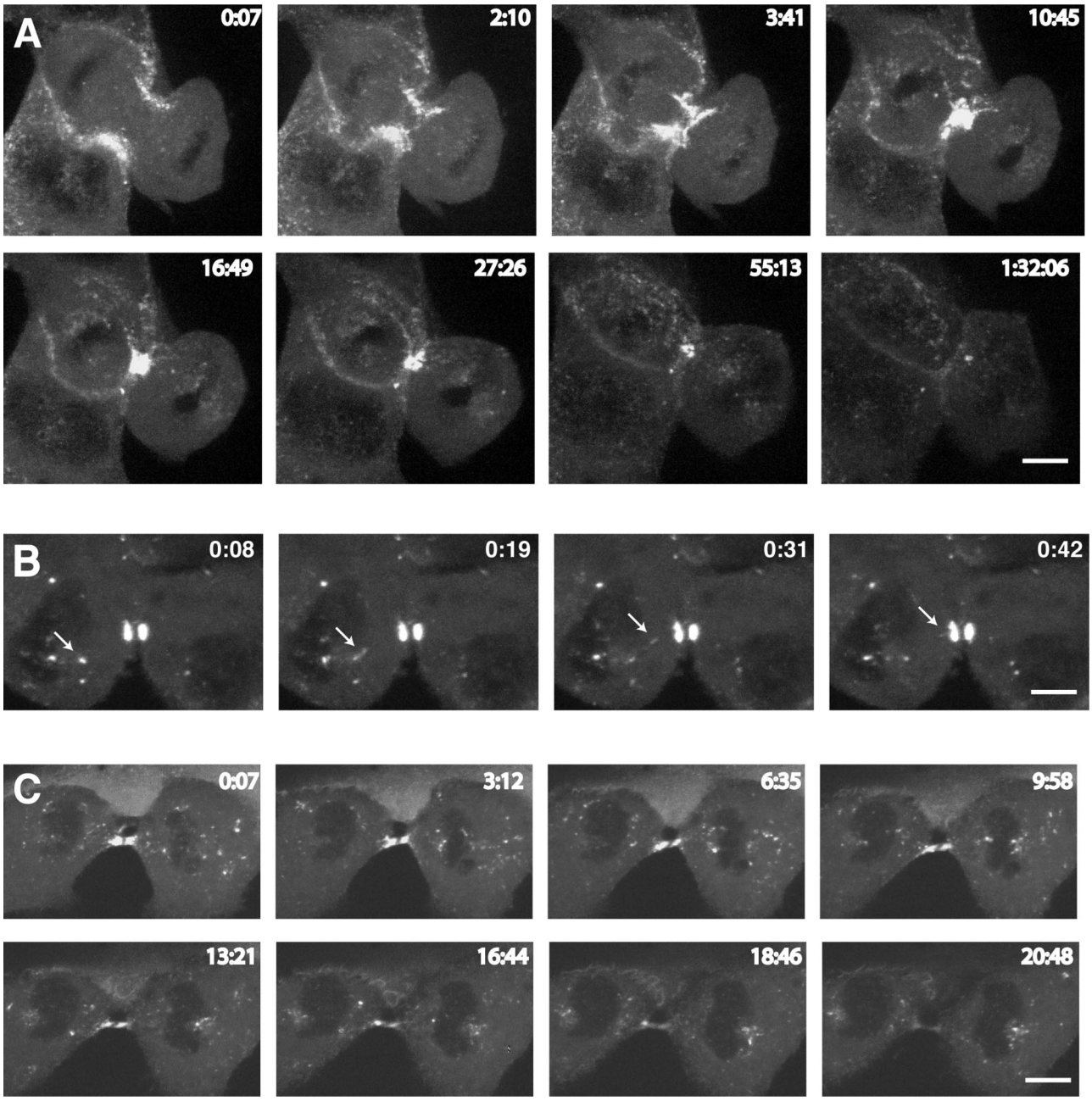

Figure 3. Spatial and temporal dynamics of GFP-myosin VI during cytokinesis. To visualize the dynamic behavior of myosin VI during mitosis, MDCK cells stably expressing GFP-myosin VI were imaged using time-lapse microscopy. (A) Gallery of still images of a cell progressing through cytokinesis (see Supplemental Movie 1). (B) A cell in late cytokinesis is shown, highlighting the presence of myosin VI on a vesicle (arrow) moving into the cleavage furrow (see Supplemental Movie 2). (C) Still images of a cell in late cytokinesis show that myosin VI-containing vesicles concentrate on either side of the midbody region and in the polar region around the spindle poles (see Supplemental Movie 3).

rapidly in 30 s into the midbody region. In this movie, equal numbers of myosin VI-positive spots are moving into and out of the cleavage furrow. This movement of myosin VI-containing punctate structures is not only observed in the cleavage furrow but also a large number of myosin VI-positive dots are moving in and out of the polar region around the spindle poles and around the perinuclear region adjacent to the cleavage furrow (Figure 3C and Supplemental Movie 3). In some cells, myosin VI-positive dots were observed moving on a fixed possible cytoskeletal track between the polar region and the cleavage furrow (Supplemental Movie 4). Unfortunately, we were unable to investigate the nature of this very intriguing but delicate track, because we were unable to visualize this track in cells after fixation. During late cytokinesis when the intercellular bridge is lengthening myosin VI-positive spots now move predominantly away from the midbody into the cell (Supplemental Movie 5). At this time myosin VI may transport endocytic vesicles out of the cytoplasmic bridge and into the cell, because it was recently reported (Schweitzer *et al*., 2005)

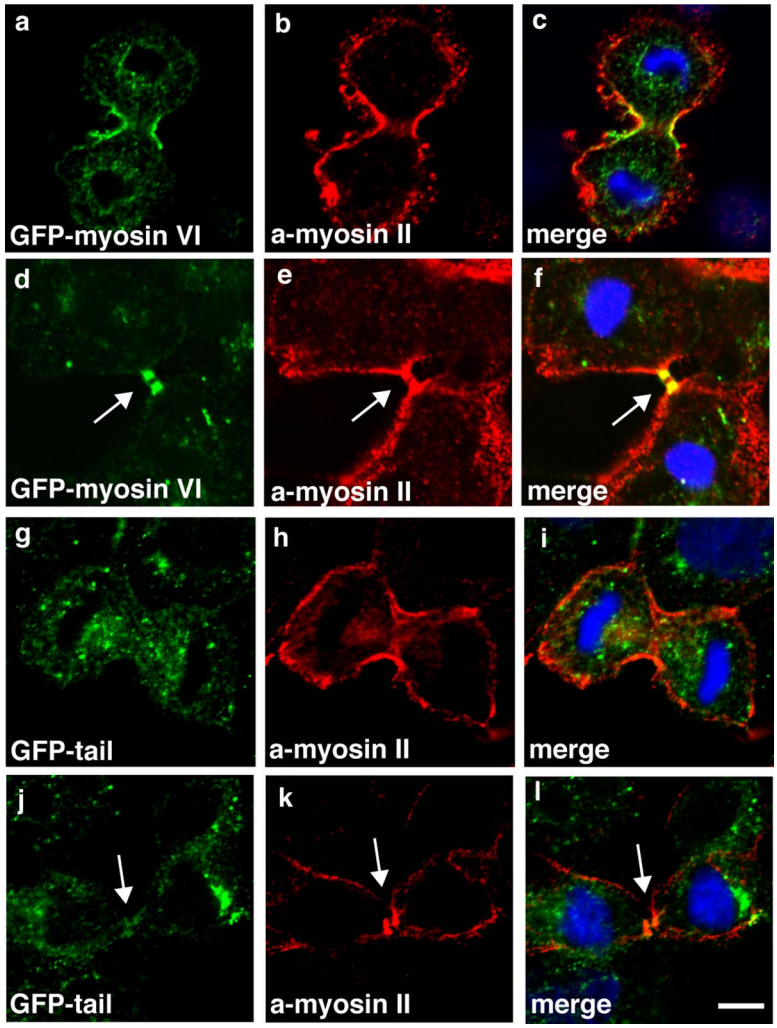

Figure 4. The myosin VI dominant-negative tail is not recruited into the cleavage furrow or the midbody region. To compare the targeting of full-length myosin VI or only the tail domain during cytokinesis, stable MDCK cells expressing full-length GFP-myosin VI (a and d) or the GFP-tail (g and j) were double labeled with a GFP-mAb and a nonmuscle myosin II polyclonal antibody (b, e, h, and k). The merged images are shown (in c, f, i, and l), and they clearly indicate that the myosin VI tail is not recruited to the walls of the ingressing cleavage furrow or the midbody region. In contrast, in both of these regions full-length myosin VI shows very good colocalization with myosin II. Arrows indicate midbody region. Bars, 10 μm.

that endocytosis resumes in late cytokinesis in the midbody region.

Our observations on the dynamic behavior of GFP-myosin VI in live cells suggests that myosin VI is involved in trafficking of vesicles into and out of the cleavage furrow during cytokinesis.

The Myosin VI Tail Is Not Targeted into the Cleavage Furrow

Previously, we showed that the intracellular localization of myosin VI to vesicular structures in the endocytic and secretory pathways requires the C-terminal cargo-binding domain (Buss *et al*., 2001; Warner *et al*., 2003; Sahlender *et al*., 2005). The targeting of myosin VI to membrane compartments is mediated by several different binding partners or by interaction with phospholipids (Spudich *et al*., 2007). Whereas the tail domain is sufficient for targeting to clathrin-coated structures at the plasma membrane, the recruitment of myosin VI into membrane ruffles at the leading edge of moving cells also requires its motor domain (Buss *et al*., 1998).

To establish whether the tail domain of myosin VI is sufficient for targeting into the cleavage furrow during cytokinesis, we compared the localization of full-length GFP-myosin VI and the GFP-tail in a double-labeling experiment with a polyclonal antibody to nonmuscle myosin II to visualize the contractile ring, because we observed that both myosin II and actin are concentrated in the intercellular bridge of MDCK cells (Figures 1 and 4 and Supplemental Figure 3). Whereas the full-length myosin VI shows very good colocalization with myosin II in the contractile ring in the ingressing cleavage furrow (Figure 4, a–c) and afterward in the midbody region (Figure 4, d–f), the GFP-tail showed no cytokinesis-specific labeling pattern (Figure 4, g–i and j–l). The tail domain was targeted to punctate, vesicular structures in dividing cells (Figure 4, g and j), which were often concentrated in the polar regions surrounding the spindle poles (Figure 7g), but no colocalization with myosin II in the cleavage furrow or the midbody region was observed (Figure 4, g and h, j and k).

Inhibition of Myosin VI Activity Delays Mitotic Progression and Leads to Cytokinesis Defects

To probe the function of myosin VI during cell division, we used two different approaches. First we inhibited myosin VI activity by overexpressing a dominant-negative tail mutant of myosin VI in MDCK cells. We used MDCK cell lines that have been generated and characterized recently (Au *et al*., 2007) and in which protein expression can be induced by addition of $ZnCl_2$. A dominant-negative approach has been used successfully to inhibit myosin VI-dependent functions in the endocytic and exocytic pathway (Buss *et al*., 2001;

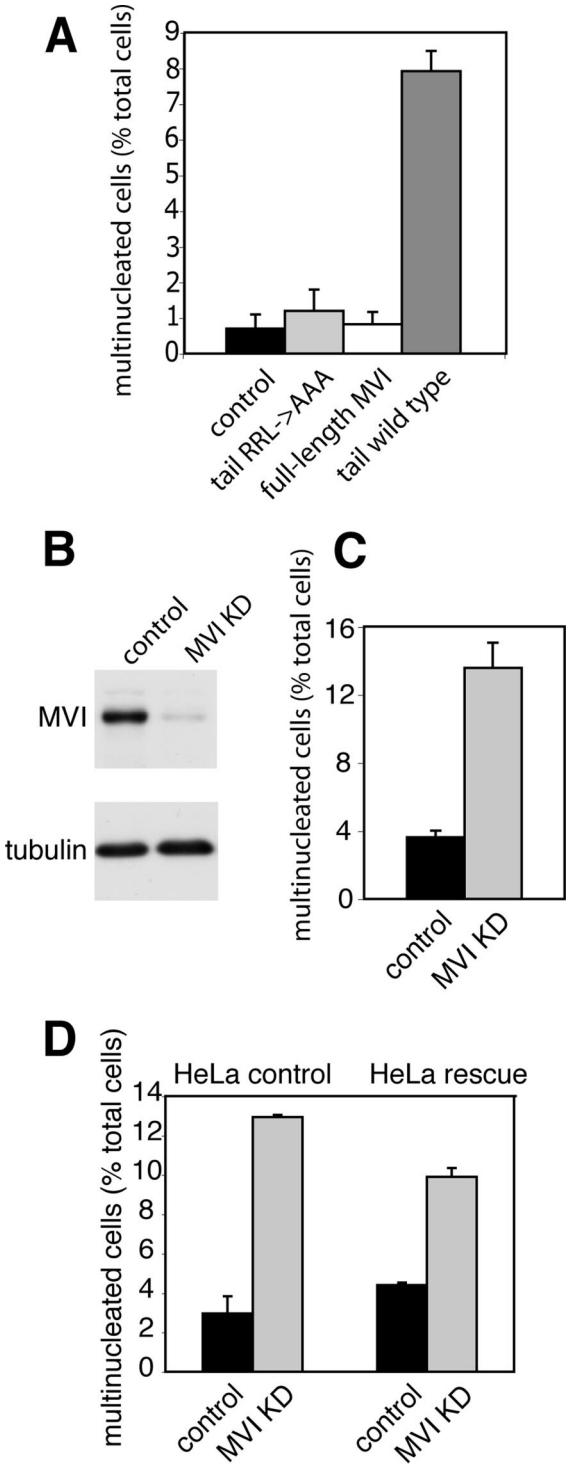

Figure 5. Loss of Myosin VI causes defects in late cytokinesis. To investigate the role of myosin VI during cytokinesis, wild-type MDCK cells (control) and stable MDCK cell lines expressing either GFP-myosin VI (full-length MVI), GFP-tail (tail wild type), or the GFP-tail with the RRL->AAA mutation (aa 1107–1109) (tail RRL->AAA) were fixed and stained with anti-tubulin antibodies and Hoechst DNA dye. To score the number of multinucleated cells, >2000 interphase cells for each condition were counted using a fluorescence microscope, and the results were plotted as a percentage of the total number of cells (A). Cytokinesis defects in myosin VI KD cells were quantified in HeLa cells that were either mock transfected or transfected with a siRNA SMARTpool specific for myosin VI. After two successive knockdowns, myosin VI protein expression was down to <10% as shown by immunoblotting (B). To quantify cytokinesis defects KD and control cells were fixed and stained with anti-tubulin antibodies and Hoechst DNA dye. The number of multinucleated cells was expressed as a percentage of total cells (C). More than 4000 cells were counted for each condition. (D) For siRNA rescue experiments knockdowns were performed in a HeLa cell line expressing an siRNA-resistant version of myosin VI (HeLa rescue). Numbers of multinucleated cells were quantified as described in C, and they were compared with control HeLa cells. Whereas in wild-type HeLa cells the absence of myosin VI leads to a more than fourfold increase in multinucleation (3–13%), the cell line expressing siRNA-resistant myosin VI only shows a twofold increase in multinucleation (from 4.5 to 9.5%), indicating a 50% rescue resulting from myosin VI expression. More than 2000 cells were counted for each condition.

Swiatecka-Urban *et al*., 2004; Au, 2007). To quantify defects in cytokinesis caused by overexpression of the dominant-negative tail mutant, we induced expression of the myosin VI wild-type tail, myosin VI tail mutant (with a mutation RRL->AAA that affects GIPC binding) or full-length myosin VI for 24–36 h, and we compared the number of multinucleated cells with wild-type MDCK cells (control) (Figure 5A). Only overexpression of the dominant-negative wild-type tail gave a significant and consistent eightfold increase in the number of multinucleated cells (<1–8%), thereby demonstrating an increase in cytokinesis failure. The mutant myosin VI tail, however, with the amino acid change (RRL to AAA; aa 1107–1109) that abolishes optineurin and GIPC binding is no longer able to block GIPC-mediated myosin VI function; therefore, it does not cause any increase in multinucleation (Figure 5A). As a second approach to manipulate myosin VI function, we used siRNA oligonucleotides to silence myosin VI expression. For these experiments, we changed from MDCK to HeLa cells, which give much higher siRNA transfection rates, and siRNA SMARTpools are easily obtainable for all human genes. These cells were transfected with a SMARTpool containing four different siRNAs specific for myosin VI. After transfection myosin VI, expression levels were down to <10% as demonstrated by Western blotting (Figure 5B). When compared with mock-treated control cells siRNA treatment did not affect cell viability significantly and the mitotic index of control and KD cells was ~2% (data not shown). Depletion of myosin VI from HeLa cells by using the SMARTpool siRNA led to a significant increase in the number of bi- and multinucleated cells (13%) compared with mock-transfected cells (3%), indicating a four- to fivefold increase in cells with defects in cytokinesis (Figure 5C). To exclude off-target effects, we performed rescue experiments in a stable HeLa cell line expressing siRNA-resistant myosin VI, and we observed 4.5% multinucleated cells when these cells were mock transfected and 10% multinucleated cells when transfected with myosin VI siRNA. This indicates only a twofold increase in multinucleation compared with wild-type HeLa cells, where the loss of myosin VI leads to a more than fourfold increase in multinucleation. Therefore, the expression of siRNA-resistant myosin VI leads to a 50% rescue of the cytokinesis defect (Figure 5D).

Loss of Myosin VI Causes a Defect in Late Cytokinesis during Final Abscission

Defects in cytokinesis can occur at different stages, either as a failure in furrow ingression or a defect in the final abscission process. To evaluate at which stage of cytokinesis loss

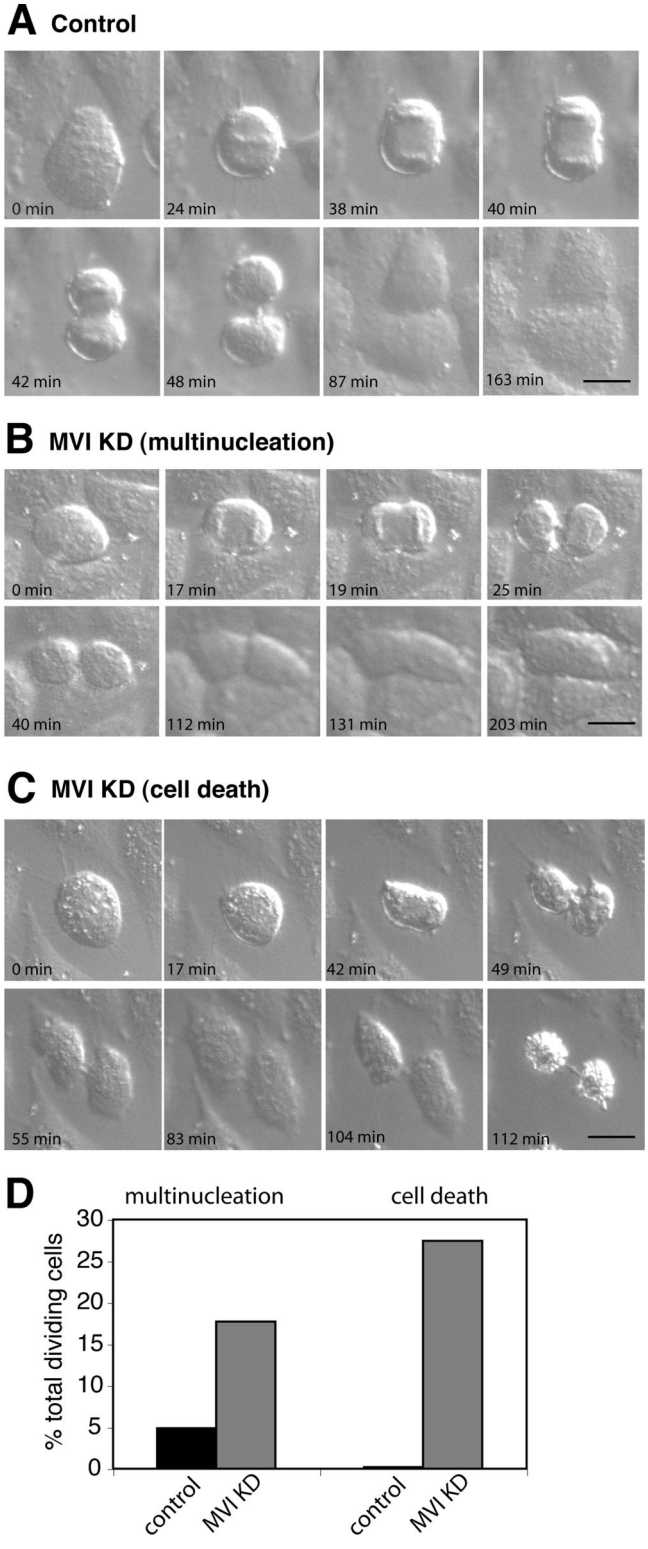

Figure 6. DIC live cell microscopy of myosin VI KD cells characterizes defects in cytokinesis. To visualize how HeLa cells lacking myosin VI are progressing through cytokinesis, control and myosin VI KD cells were imaged using time-lapse DIC microscopy. A gallery of still images of a mock-transfected control cell progressing through cytokinesis is shown in A (see Supplemental Movie 6). (B) Representative series of images of a myosin VI KD cell forming a cleavage furrow that later on regresses to form a binucleated cell (see Supplemental Movie 7). (C) Gallery of images following a cell through cytokinesis; the cell fails to complete abscission and forms two apoptotic daughter cells connected by a thin cytoplasmic bridge (see Supplemental Movie 8). To quantify these defects, the number of multinucleated and dead cells was counted and expressed as a percentage of the total number of dividing cells (D). In total, 41 control and 62 myosin VI KD cells were analyzed and counted. Bars, 20 μm.

of myosin VI leads to the formation of multinucleated cells, we used DIC time-lapse videomicroscopy. HeLa cell were treated with myosin VI SMARTpool siRNA primers, and 24 h after the last transfection, cells in early metaphase were chosen as a starting point to monitor progression through cytokinesis. In Figure 6, still images of a time-lapse movie of control (A) and myosin VI KD HeLa cells (B and C) are shown (see also Supplemental Movies 6–8). Live cell imaging of the myosin VI KD cells identified two major phenotypes: 1) the KD cells established a cleavage furrow and the cleavage furrow constricted into a narrow bridge, but later regresses without separation and the cell becomes binucleated (Figure 6B); and 2) the cell forms a deeply invaginated cleavage furrow, which does not regress, and the two daughter cells spread out. However, no abscission takes place and both daughter cells die while still connected by a thin cytoplasmic bridge (Figure 6C). In total, 41 control movies and 62 movies of myosin VI KD cells were analyzed and quantified. Sixteen percent of KD cells formed a binucleated cell, which confirms our results on fixed KD cells. In 25% of KD cells, the loss of myosin VI led to abscission failure and cell death (Figure 6D). Therefore, in total, 41% of myosin VI KD cells show defects in cytokinesis leading either to multinucleation (16%) or to cell death (25%).

Finally, we also observed a significant increase in the number of cells in metaphase, when myosin VI was depleted by siRNA, suggesting that progression through metaphase was delayed (Supplemental Figure 1). To further investigate this result, we followed mock-treated and KD cells through mitosis by using DIC microscopy. In HeLa control cells, >95% of cells (n = 23) proceeded into anaphase within 30 min after the cells had started to assemble chromosomes at the metaphase plate. In myosin VI KD cells, however, nearly all the cells took >30 min to go through metaphase and to enter anaphase and 70% of the cells (N = 24) took >60 min to reach anaphase. These results suggest that myosin VI may also play a role in chromosome alignment during metaphase.

Myosin VI Mediates the Insertion of TfR-containing Endosomes into the Midbody Region

The insertion of membranes from the endocytic and secretory pathway into the cleavage furrow is crucial for successful completion of cytokinesis. Because myosin VI has been localized in clathrin-coated and -uncoated endocytic structures (Buss *et al*., 2001) (Aschenbrenner *et al*., 2003), we next examined whether myosin VI is involved in delivery of endocytic material into the cleavage furrow. In MDCK cells expressing GFP-myosin VI or GFP-myosin VI tail, we labeled the endocytic compartment with an antibody to the transferrin receptor. This receptor is taken up into mammalian cells via clathrin-mediated endocytosis and after passing through a recycling endosome, it is trafficked back to the cell surface or into the midbody region. GFP-myosin VI and GFP-myosin VI tail both showed very good colocalization with the transferrin receptor positive compartment, possibly the recycling endosome, in the region around the spindle pole (Figure 7, a–c, and g–i, arrowheads). However, in the midbody region, we only observed colocalization between

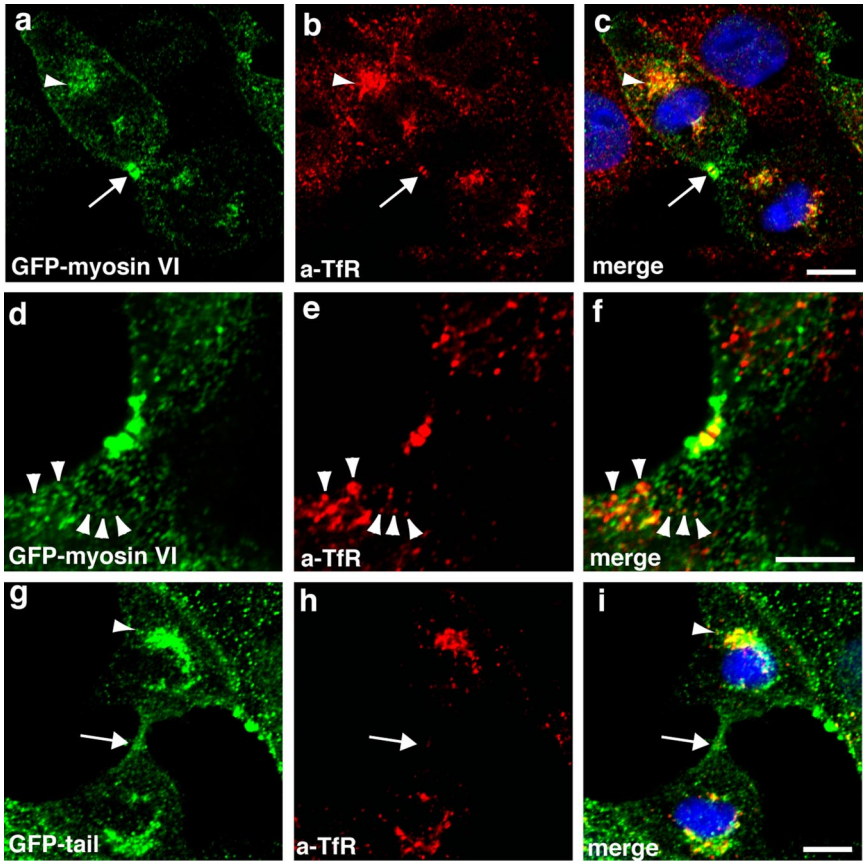

Figure 7. Overexpression of the dominant-negative myosin VI tail inhibits transport of TfR into the midbody region. Stable MDCK cells expressing full-length GFP-myosin VI (a and d) or only the GFP-tail domain (g) were double labeled in indirect immunofluorescence with a mAb to the TfR (b, e, and h). Full-length GFP-myosin VI colocalizes with the TfR that is concentrated in the polar region (a–c, arrowhead) around the spindle pole and in the midbody region (a–c, arrow). Arrowheads mark single TfR-positive vesicles (d–f) that contain myosin VI. In cells overexpressing the myosin VI tail, the TfR is still present in the polar region, and it is not present in the midbody region (arrow, g–i). Bars, 10 μm.

full-length myosin VI and the TfR (Figure 7 a–c, arrow), because in cells expressing GFP-myosin VI tail there was no TfR and very little myosin VI tail was detected in the midbody region (Figure 7, g–i). Our confocal images also demonstrated limited but significant colocalization of GFP-myosin VI with TfR positive endosomes in close vicinity to the midbody region (Figure 7, d–f, arrowheads), which might represent the myosin VI-positive vesicle population moving into and out of the cytoplasmic bridge that we observed in our live cell studies. These results indicate that the myosin VI tail domain is able to inhibit as a dominant-negative mutant the transport of TfR-positive endocytic vesicles into the midbody region.

Finally, we investigated whether myosin VI is also associated with the secretory pathway during cytokinesis, because in interphase cells myosin VI can be found at the Golgi complex and in exocytic membrane-trafficking pathways. During cytokinesis, however, very little myosin VI was associated with the Golgi fragments in the polar region stained with antibodies to the Golgi matrix protein GM130 (Supplemental Figure 2). Furthermore, no colocalization of myosin VI with GM130 or proteins involved in post-Golgi membrane trafficking in the midbody region was observed (Supplemental Figure 2).

GIPC Colocalizes with Myosin VI in the Midbody Region and Loss of GIPC Results in Increased Number of Multinucleated Cells

Targeting of myosin VI to distinct intracellular compartments requires binding to several different binding partners. The study by Skop *et al*. (2004) indicated that not only myosin VI but also GIPC, a myosin VI binding partner, is present in isolated midbodies. GIPC, a small PDZ domain-containing protein, colocalizes with myosin VI on endocytic vesicles (Aschenbrenner *et al*., 2003), and it has been shown to bind to a number of transmembrane receptors at the cell surface and the Golgi complex in interphase cells (Katoh, 2002). Using polyclonal antibodies to GIPC, we observed a striking localization of GIPC on either side of the midbody region colocalizing with GFP-tagged myosin VI in MDCK cells (Figure 8, d–f). There was a perfect overlap between myosin VI and GIPC in the midbody region and on vesicular structures on either side of the cleavage furrow (Figure 8, g–i). In addition, both proteins were recruited to the walls of the cleavage furrow during late anaphase/telophase (Figure 8, a–c). These results strongly suggest that a complex between myosin VI and GIPC may be essential for myosin VI to function during cytokinesis. This finding is supported by the observation that the myosin VI tail, where the GIPC binding site is mutated (RRL to AAA) (Spudich *et al*., 2007) has no dominant-negative inhibitory effect on the function of myosin VI during cytokinesis (Figure 5A).

To investigate the role of GIPC in dividing cells, we used a GIPC SMARTpool to ablate GIPC expression in HeLa cells. Immunoblotting analysis indicated that transfection with GIPC siRNA oligos very efficiently depleted the expression of GIPC (Figure 8B). In GIPC KD cells, we observed a more than fourfold increase in the number of multinucleated cells (13%) compared with mock-transfected HeLa cells (3%) (Figure 8C). These results indicate that the loss of GIPC and myosin VI both lead to defects in cytokinesis, and they suggest that both proteins might be involved in the final abscission step in cell division.

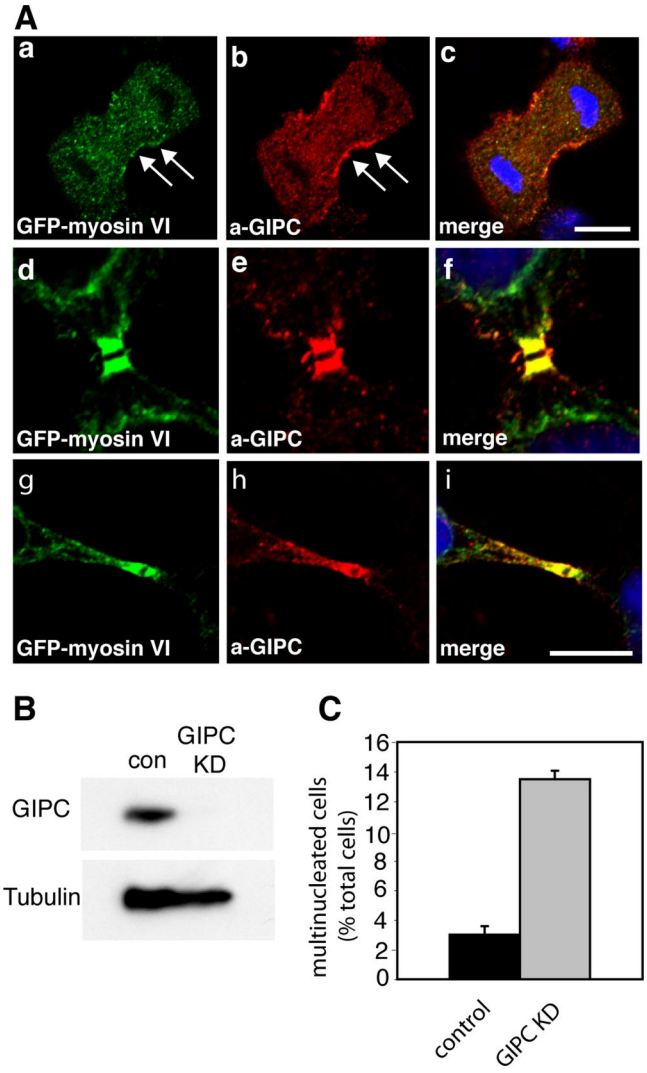

Figure 8. Myosin VI colocalizes with GIPC in dividing cells, and the loss of GIPC causes defects in cytokinesis. (A) MDCK cells stably expressing GFP-myosin VI were labeled with a GFP-antibody (a, d, and g) and with a GIPC antibody (b, e, and h). The merged images together with the DNA stain in blue are shown in c, f, and i. Myosin VI and GIPC are both recruited to the ingressing cleavage furrow in late anaphase/telophase (arrows in a and b), and they show perfect colocalization in the midbody region in late cytokinesis (d–i). Bars, 10 μm. (B) Western blot showing GIPC expression levels in mock-treated control cells and GIPC KD cells transfected with a SMARTpool of siRNA specific for GIPC. An α-Tubulin blot is shown as a loading control. After two knockdowns (72 h), no GIPC can be detected by immunoblotting. (C) HeLa grown on coverslips were transfected twice with SMARTpool siRNA specific for GIPC. Twenty-four hours after the second transfection, the cells were fixed and stained with Hoechst DNA dye. The number of multinucleated cells was counted and expressed as a percentage of the total number of cells. More than 2500 cells were counted for each condition.

DISCUSSION

In this study, we have shown that in dividing cells myosin VI has novel roles during both mitosis and cytokinesis. In cells undergoing cell division, we show that myosin VI at the beginning of prophase is concentrated around the centrosome, whereas during cytokinesis myosin VI is present on the walls of the ingressing cleavage furrow and on vesicles moving into and out of the midbody region, where the myosin VI binding partner GIPC can also be found. The loss of myosin VI function induced by siRNA oligonucleotides or by dominant-negative overexpression of the tail leads to defects in cytokinesis. In addition, we also observed a delay in chromosome congression at the metaphase plate, highlighting an unexpected function of myosin VI during spindle assembly and chromosome gathering. Although these latter events were generally thought to be microtubule-driven processes, it was recently demonstrated that in oocytes a contractile network of actin filaments captures chromosomes and brings them close to the spindle for microtubule attachment (Lenart *et al*., 2005). Overall the role of actin filaments in chromosome capture and congression may not be restricted to large oocytes; it also may operate in other smaller somatic cells undergoing mitosis. In these cells, an increasing number of actin-regulating proteins, such as the Rho GTPase cdc42 and its effector mDia, have been shown to be important for cell cycle progression (Yasuda *et al*., 2004). These proteins induce actin filament nucleation and polymerization and they regulate microtubule attachment to kinetochores and chromosome alignment at the metaphase plate. Therefore, it may not come as a surprise that myosin VI, a unique actin-based motor protein, is recruited to centrosomes/spindle poles during prophase.

However, the loss of myosin VI in knockdown cells does not lead to a complete mitotic arrest. In addition in fibroblasts isolated from the myosin VI knockout mouse (Snell's waltzer mouse), no major defects in chromosome alignment or spindle morphology were observed. These results suggest that redundant pathways exist for spindle assembly and chromosome congression in mammalian cells. The prometaphase delay in myosin VI knockdown cells is very similar to the delay described recently for Clip 170 KD cells (Dujardin *et al*., 1998; Tanenbaum *et al*., 2006). Clip 170 was identified as a myosin VI binding partner in *Drosophila* (Lantz and Miller, 1998); however, in mammalian cells we have not been able to confirm by yeast two-hybrid or mammalian two-hybrid assays or by coimmunoprecipitation any interaction between myosin VI and Clip 170. So far, we were only able to demonstrate direct binding of Clip 170 to myosin VI in a glutathione transferase pull-down assay using recombinant GST tagged myosin VI tail and in vitro expressed Clip 170 (data not shown).

The midbody has a complex multicomponent structure that forms between dividing cells during cytokinesis. A recent proteomics study identified myosin VI and GIPC as mammalian midbody proteins and highlighted a role for these two proteins in germline cytokinesis in *C. elegans* (Skop *et al*., 2004). We have confirmed the localization of GIPC in the midbody region in mammalian cells; furthermore, we have shown that in siRNA knockdown experiments, the loss of GIPC leads to a dramatic failure in cytokinesis, resulting in binucleated and multinucleated cells. Detailed immunolocalization studies show that GIPC is concentrated on either side of the midbody, and in double-labeling experiments, GIPC shows a dramatic overlap with myosin VI in the cleavage furrow on either side of the midbody.

Membrane trafficking is an essential part of cytokinesis for delivering and regulating the addition of new membrane along the ingressing cleavage furrow (Strickland and Burgess, 2004; Albertson *et al*., 2005). The importance of membrane fusion events during cytokinesis is highlighted by the requirement of soluble *N*-ethylmaleimide-sensitive factor attachment protein receptor proteins (Low *et al*., 2003). The new membrane delivered into the cleavage furrow may be derived from the secretory, endocytic, or recycling pathways. In some cell systems, brefeldin A inhibits cytokinesis,

indicating that Golgi-derived membrane trafficking is involved (Skop *et al*., 2001). Furthermore, proteomic analysis of mammalian midbodies identified a number of Golgi-derived proteins (Skop *et al*., 2004). Because myosin VI plays a role in exocytic membrane trafficking pathways, it could be involved together with its binding partner optineurin in transporting Golgi-derived vesicles into the midbody region (Warner *et al*., 2003; Sahlender *et al*., 2005). However, so far we have not observed any colocalization of myosin VI with any Golgi fragments in dividing cells or any targeting of optineurin into the cleavage furrow during cytokinesis. Furthermore, depletion of optineurin by siRNA does not result in a cytokinesis defect and multinucleation. These results indicate that myosin VI is apparently not involved in the transport of secretory vesicles into the midbody area.

Endocytosis and membrane recycling are, however, crucial for cytokinesis, because proteins essential for these processes, such as clathrin, caveolin, dynamin, Arf6, and Rab11, are required (Kogo and Fujimoto, 2000; Gerald *et al*., 2001; Schweitzer and D'Souza-Schorey, 2002). Recently, it has been shown that in early telophase, endocytosis resumes at the polar regions of the dividing cell (Schweitzer *et al*., 2005). In this study, it was demonstrated that endocytosed transferrin accumulates first in vesicles around the spindle poles, and then these vesicles are transported to the cleavage furrow in late cytokinesis. Given the localization of myosin VI in vesicles surrounding the spindle poles and in vesicles moving into the midbody region, myosin VI is most likely to be a driving force for the transport of vesicles from the pericentriolar vesicular compartment into the cleavage furrow, because inhibition of myosin VI function dramatically reduces the amount of TfR-containing vesicles transported into the midbody region. The tail domain of myosin VI targets to vesicles in the pericentriolar region but not to the cleavage furrow, indicating that the dominant-negative tail inhibits the formation and/or transport of vesicles away from the pericentriolar recycling/sorting endosome. Although the exact nature of this pericentriolar compartment needs to be established, our previous work has shown that ablating myosin VI function in polarized MDCK cells perturbs the correct sorting of cargo to the basolateral domain (Au *et al*., 2007). This sorting step is thought to involve the transferrin-positive recycling endosome, which may be a very similar compartment to that in the pericentriolar region in cells undergoing cytokinesis.

In the final stages of cytokinesis, our live cell movies indicate that myosin VI-containing vesicles not only move into the cleavage furrow but also predominately move away from the midbody back into the cell. Because work by Schweitzer *et al*. (2005) has shown that endocytosis resumes from the midbody region at the end of cytokinesis, it is likely that at this stage myosin VI may be transporting endocytic membranes back into the cell.

During cytokinesis, actin filaments assemble not only as a circumferential belt as part of the contractile ring but also align themselves along the spindle axis in a complex three-dimensional network (Fishkind and Wang, 1993). Although the polarity of these actin filaments is not known, there is an obvious need for a reverse-directed motor such as myosin VI; however, at present, its precise function has not been identified.

The movement of myosin VI to the centrosome in early mitosis and into the cleavage furrow and the midbody region seems to involve interaction with specific binding partners such as GIPC. A minor mutation (RRL->AAA) prevents GIPC binding to the myosin VI tail (Spudich *et al*., 2007), and it abolishes the ability of the tail to cause cytokinesis defects. Targeting of myosin VI to the ingressing cleavage furrow might also involve its high-affinity binding site for PIP_2 in the C-terminal tail domain (Spudich *et al*., 2007), which we have recently identified. Several studies have recently shown that PIP_2 accumulates at the cleavage furrow and that its presence is necessary for successful furrow ingression during cytokinesis (Emoto *et al*., 2005; Field *et al*., 2005; Janetopoulos *et al*., 2005; Janetopoulos and Devreotes, 2006).

The dual localization of myosin VI in dividing cells at and around the centrosome in early mitosis and later in the midbody region during cytokinesis is very intriguing, and future experiments will be required to determine whether myosin VI displays separate independent functions during prometaphase at the centrosome and during cytokinesis or whether it is part of the signaling networks that coordinate or regulate mitosis, cytokinesis, and abscission.

ACKNOWLEDGMENTS

We thank Dr. M. Chibalina for critical reading of the manuscript. This work was funded by a Wellcome Trust Senior Fellowship (to F.B.), a Cancer Research UK project grant (to C.P.), a Croucher Foundation Research Studentship (to J.A.), and it was supported by the Medical Research Council. Cambridge Institute for Medical Research is in receipt of a strategic award from the Wellcome Trust.

REFERENCES

Albertson, R., Riggs, B., and Sullivan, W. (2005). Membrane traffic: a driving force in cytokinesis. Trends Cell Biol. *15*, 92–101.

Aschenbrenner, L., Lee, T., and Hasson, T. (2003). Myo6 facilitates the translocation of endocytic vesicles from cell peripheries. Mol. Biol. Cell *14*, 2728–2743.

Au, J., Puri, C., Ihrke, G., Kendrick-Jones, J., Buss, F. (2007). Myosin VI is required for sorting of AP-1B dependent cargo to the basolateral domain in polarised MDCK cells. J. Cell Biol. *177*, 103–114.

Bunn, R. C., Jensen, M. A., and Reed, B. C. (1999). Protein interactions with the glucose transporter binding protein GLUT1CBP that provide a link between GLUT1 and the cytoskeleton. Mol. Biol. Cell *10*, 819–832.

Buss, F., Arden, S. D., Lindsay, M., Luzio, J. P., and Kendrick-Jones, J. (2001). Myosin VI isoform localized to clathrin-coated vesicles with a role in clathrin-mediated endocytosis. EMBO J. *20*, 3676–3684.

Buss, F., Kendrick-Jones, J., Lionne, C., Knight, A. E., Cote, G. P., and Paul Luzio, J. (1998). The localization of myosin VI at the Golgi complex and leading edge of fibroblasts and its phosphorylation and recruitment into membrane ruffles of A431 cells after growth factor stimulation. J. Cell Biol. *143*, 1535–1545.

Buss, F., Spudich, G., and Kendrick-Jones, J. (2004). Myosin VI: cellular functions and motor properties. Annu. Rev. Cell Dev. Biol. *20*, 649–676.

De Vries, L., Lou, X., Zhao, G., Zheng, B., and Farquhar, M. G. (1998). GIPC, a PDZ domain containing protein, interacts specifically with the C terminus of RGS-GAIP. Proc. Natl. Acad. Sci. USA *95*, 12340–12345.

Drenckhahn, D., Groschel-Stewart, U., Kendrick-Jones, J., and Scholey, J. M. (1983). Antibody to thymus myosin: its immunological characterization and use for immunocytochemical localization of myosin in vertebrate nonmuscle cells. Eur. J. Cell Biol. *30*, 100–111.

Dujardin, D., Wacker, U. I., Moreau, A., Schroer, T. A., Rickard, J. E., and De Mey, J. R. (1998). Evidence for a role of CLIP-170 in the establishment of metaphase chromosome alignment. J. Cell Biol. *141*, 849–862.

Emoto, K., Inadome, H., Kanaho, Y., Narumiya, S., and Umeda, M. (2005). Local change in phospholipid composition at the cleavage furrow is essential for completion of cytokinesis. J. Biol. Chem. *280*, 37901–37907.

Field, S. J., Madson, N., Kerr, M. L., Galbraith, K. A., Kennedy, C. E., Tahiliani, M., Wilkins, A., and Cantley, L. C. (2005). PtdIns(4,5)P2 functions at the cleavage furrow during cytokinesis. Curr. Biol. *15*, 1407–1412.

Fielding, A. B., Schonteich, E., Matheson, J., Wilson, G., Yu, X., Hickson, G. R., Srivastava, S., Baldwin, S. A., Prekeris, R., and Gould, G. W. (2005). Rab11-FIP3 and FIP4 interact with Arf6 and the exocyst to control membrane traffic in cytokinesis. EMBO J. *24*, 3389–3399.

Fishkind, D. J., and Wang, Y. L. (1993). Orientation and three-dimensional organization of actin filaments in dividing cultured cells. J. Cell Biol. *123*, 837–848.

Gerald, N. J., Damer, C. K., O'Halloran, T. J., and De Lozanne, A. (2001). Cytokinesis failure in clathrin-minus cells is caused by cleavage furrow instability. Cell Motil. Cytoskeleton *48*, 213–223.

Glotzer, M. (2005). The molecular requirements for cytokinesis. Science *307*, 1735–1739.

Janetopoulos, C., Borleis, J., Vazquez, F., Iijima, M., and Devreotes, P. (2005). Temporal and spatial regulation of phosphoinositide signaling mediates cytokinesis. Dev. Cell *8*, 467–477.

Janetopoulos, C., and Devreotes, P. (2006). Phosphoinositide signaling plays a key role in cytokinesis. J. Cell Biol. *174*, 485–490.

Katoh, M. (2002). GIPC gene family. Int. J. Mol. Med. *9*, 585–589.

Kogo, H., and Fujimoto, T. (2000). Concentration of caveolin-1 in the cleavage furrow as revealed by time-lapse analysis. Biochem. Biophys. Res. Commun. *268*, 82–87.

Lantz, V. A., and Miller, K. G. (1998). A class VI unconventional myosin is associated with a homologue of a microtubule-binding protein, cytoplasmic linker protein-170, in neurons and at the posterior pole of *Drosophila* embryos. J. Cell Biol. *140*, 897–910.

Lenart, P., Bacher, C. P., Daigle, N., Hand, A. R., Eils, R., Terasaki, M., and Ellenberg, J. (2005). A contractile nuclear actin network drives chromosome congression in oocytes. Nature *436*, 812–818.

Low, S. H., Li, X., Miura, M., Kudo, N., Quinones, B., and Weimbs, T. (2003). Syntaxin 2 and endobrevin are required for the terminal step of cytokinesis in mammalian cells. Dev. Cell *4*, 753–759.

Morris, S. M., Arden, S. D., Roberts, R. C., Kendrick-Jones, J., Cooper, J. A., Luzio, J. P., and Buss, F. (2002). Myosin VI binds to and localises with Dab2, potentially linking receptor-mediated endocytosis and the actin cytoskeleton. Traffic *3*, 331–341.

Morris, S. M., and Cooper, J. A. (2001). Disabled-2 colocalizes with the LDLR in clathrin-coated pits and interacts with AP-2. Traffic *2*, 111–123.

Sahlender, D. A., Roberts, R. C., Arden, S. D., Spudich, G., Taylor, M. J., Luzio, J. P., Kendrick-Jones, J., and Buss, F. (2005). Optineurin links myosin VI to the Golgi complex and is involved in Golgi organization and exocytosis. J. Cell Biol. *169*, 285–295.

Scholey, J. M., Brust-Mascher, I., and Mogilner, A. (2003). Cell division. Nature *422*, 746–752.

Schweitzer, J. K., Burke, E. E., Goodson, H. V., and D'Souza-Schorey, C. (2005). Endocytosis resumes during late mitosis and is required for cytokinesis. J. Biol. Chem. *280*, 41628–41635.

Schweitzer, J. K., and D'Souza-Schorey, C. (2002). Localization and activation of the ARF6 GTPase during cleavage furrow ingression and cytokinesis. J. Biol. Chem. *277*, 27210–27216.

Skop, A. R., Bergmann, D., Mohler, W. A., and White, J. G. (2001). Completion of cytokinesis in *C. elegans* requires a brefeldin A-sensitive membrane accumulation at the cleavage furrow apex. Curr. Biol. *11*, 735–746.

Skop, A. R., Liu, H., Yates, J., 3rd, Meyer, B. J., and Heald, R. (2004). Dissection of the mammalian midbody proteome reveals conserved cytokinesis mechanisms. Science *305*, 61–66.

Slot, J. W., Geuze, H. J., Gigengack, S., Lienhard, G. E., and James, D. E. (1991). Immuno-localization of the insulin regulatable glucose transporter in brown adipose tissue of the rat. J. Cell Biol. *113*, 123–135.

Spudich, G., Chibalina, M. V., Au, J. S., Arden, S. D., Buss, F., and Kendrick-Jones, J. (2007). Myosin VI targeting to clathrin-coated structures and dimerization is mediated by binding to Disabled-2 and PtdIns(4,5)P(2). Nat. Cell Biol. *9*, 176–183.

Stoorvogel, W., Oorschot, V., and Geuze, H. J. (1996). A novel class of clathrin-coated vesicles budding from endosomes. J. Cell Biol. *132*, 21–33.

Strickland, L. I., and Burgess, D. R. (2004). Pathways for membrane trafficking during cytokinesis. Trends Cell Biol. *14*, 115–118.

Swiatecka-Urban, A., Boyd, C., Coutermarsh, B., Karlson, K. H., Barnaby, R., Aschenbrenner, L., Langford, G. M., Hasson, T., and Stanton, B. A. (2004). Myosin VI regulates endocytosis of the cystic fibrosis transmembrane conductance regulator. J. Biol. Chem. *279*, 38025–38031.

Tanenbaum, M. E., Galjart, N., van Vugt, M. A., and Medema, R. H. (2006). CLIP-170 facilitates the formation of kinetochore-microtubule attachments. EMBO J. *25*, 45–57.

van Dam, E. M., and Stoorvogel, W. (2002). Dynamin-dependent transferrin receptor recycling by endosome-derived clathrin-coated vesicles. Mol. Biol. Cell *13*, 169–182.

Warner, C. L., Stewart, A., Luzio, J. P., Steel, K. P., Libby, R. T., Kendrick-Jones, J., and Buss, F. (2003). Loss of myosin VI reduces secretion and the size of the Golgi in fibroblasts from Snell's waltzer mice. EMBO J. *22*, 569–579.

Wells, A. L., Lin, A. W., Chen, L. Q., Safer, D., Cain, S. M., Hasson, T., Carragher, B. O., Milligan, R. A., and Sweeney, H. L. (1999). Myosin VI is an actin-based motor that moves backwards. Nature *401*, 505–508.

Wilson, G. M., Fielding, A. B., Simon, G. C., Yu, X., Andrews, P. D., Hames, R. S., Frey, A. M., Peden, A. A., Gould, G. W., and Prekeris, R. (2005). The FIP3-Rab11 protein complex regulates recycling endosome targeting to the cleavage furrow during late cytokinesis. Mol. Biol. Cell *16*, 849–860.

Yasuda, S., Oceguera-Yanez, F., Kato, T., Okamoto, M., Yonemura, S., Terada, Y., Ishizaki, T., and Narumiya, S. (2004). Cdc42 and mDia3 regulate microtubule attachment to kinetochores. Nature *428*, 767–771.